Reprinted from **MACROMOLECULES**, Vol. *16*, Page 371, March, 1983

Effects of Annealing and Prior History on Enthalpy Relaxation in Glassy Polymers. 3. Experimental and Modeling Studies of Polystyrene

Ian M. Hodge* and Gary S. Huvard

The BFGoodrich Company, Research and Development Center, Brecksville, Ohio 44141.
Received May 5, 1982

ABSTRACT: The relaxation component of the heat capacity at constant heating rate (10 K min^{-1}) of a polydisperse polystyrene as a function of previous cooling rate, annealing time, and annealing temperature is accurately predicted by an adaptation of an algorithm due to Moynihan using parameter values determined from an analysis of the glass transition kinetics of a single thermal history. For this material, the annealing behavior below T_g is determined by the same kinetic parameters that describe the glass transition phenomenon. A similar analysis of published data for a monodisperse polystyrene indicates that the monodisperse material has a broader distribution of relaxation times and is more nonlinear. The parameter optimization method used appears to be sufficiently sensitive to permit routine characterization of the enthalpy relaxation of amorphous materials.

Introduction

Annealing of polymers below the glass transition temperature range results in a decrease in enthalpy, which is recovered during reheating to above the transition range. This recovery is manifested as an endothermic peak or inflection in the heat capacity at temperatures ranging from well below[1-7] to the upper edge[8-10] of the glass transition range. A review of experimental aspects of this phenomenon has been given by Petrie.[10] Sufficient data have now been published to permit several generalizations to be made: (1) The decrease in enthalpy during annealing, ΔH, and the temperature at which the heat capacity maximum occurs, T_{max}, are both increasing linear functions of annealing temperature T_e when T_e is more than ca. 30 K below T_g. When T_e is about 20 K below T_g, ΔH passes through a maximum and then decreases with increasing T_e. (2) ΔH and T_{max} are linear functions of log t_e (t_e = annealing time) when t_e is sufficiently short that the annealed glass is still far from equilibrium. At long t_e, ΔH becomes constant as the annealed glass approaches equilibrium. (3) Both ΔH and the value of C_p at T_{max}, C_{pmax}, increase with heating rate Q_H. T_{max} increases approximately linearly with log Q_H.

Kovacs et al.[11] and Hodge and Berens[12] have demonstrated that sub-T_g peaks result from the nonexponentiality and nonlinearity of the glass transition kinetics. Hodge and Berens also demonstrated that all of the experimental observations listed above are reproduced by applying the successful treatment of glass transition kinetics described by Moynihan and co-workers[13] to thermal histories, which included annealing. In addition, a good description of T_{max} and C_{pmax} as a function of T_e and t_e for poly(vinyl chloride) (PVC) was obtained.[12]

Although the validity of applying Moynihan's formulation to annealing effects is well supported by the reproduction of the general trends listed above, its reproduction of the data for PVC is not a good quantitative test of its accuracy for several reasons. First, the amount of "crystallinity" in the PVC (as measured by the area of the broad endotherms well above T_g) was not closely controlled, and in view of suggestions that crystallinity may immobilize chain segments in the amorphous phase at the interface,[14-16] the possibility exists that the distribution of relaxation times (or nonexponentiality) differed from one sample to another. Also, it is known that the breadth of the glass transition increases with crystallinity in several polymers,[15] and since this breadth is determined by a number of factors in addition to the distribution width (e.g., activation energy and nonlinearity), it is possible that other aspects of the glass transitions were affected as well. Second, the PVC powder was quenched into liquid nitrogen in order to accelerate the annealing process, so that the cooling rate through T_g could only be estimated. Finally, the extraction of parameters from the experimental data was performed by a subjective judgment of goodness of fit.

The work described here was motivated by the need to test the application of Moynihan's formulation to annealing more rigorously. For this purpose a completely amorphous polymer, atactic polystyrene (PS), was chosen and all cooling, annealing, and reheating were performed in the DSC instrument under controlled conditions. Model parameters were obtained from experimental data for a single thermal history by the optimization procedure described below, and the model was tested by comparing predictions for other thermal histories with experimental data. Since it was not our purpose to compare the merits of the Moynihan approach with any other description (e.g., that of Kovacs et al.[11]), other formulations were not tested.

The Model

For convenience, we give a brief account of Moynihan's treatment and how annealing is introduced. A full description is given elsewhere.[12] Enthalpy relaxation is calculated from Boltzmann superposition of responses to the total thermal history by considering cooling and

heating as a series of small temperature steps (1 K) and isothermal holds. For convenience, the enthalpy is assumed to decay according to the nonexponential function

$$\phi(t) = \exp[-(t/\tau_0)^{\beta}] \quad (1)$$

where β determines the degree of nonexponentiality ($0 < \beta \leq 1$) and τ_0 is a characteristic relaxation time that depends on both temperature and enthalpy. The latter is defined in terms of the fictive temperature, T_f, defined as the temperature at which the observed enthalpy would be the equilibrium value. The expression used for τ_0 is[17]

$$\tau_0 = A \exp\left[\frac{x\Delta h^*}{RT} + \frac{(1-x)\Delta h^*}{RT_f}\right] \quad (2)$$

where A, x, and Δh^* are parameters assumed to be independent of T and T_f, and R is the ideal gas constant. The parameter Δh^* determines how the frozen-in fictive temperature of the glass, T_f', varies with cooling rate Q_C:

$$\frac{\partial \ln Q_C}{\partial(1/T_f')} = -\Delta h^*/R \quad (3)$$

Thus, Δh^* can be determined directly from experimental data. The parameter A, together with Δh^*, largely determines the value of T_f' for a given Q_C. The parameter x is a direct measure of nonlinearity, i.e., the relative importance of T and T_f in determining the average relaxation time.

Adaptation of this treatment to include the effects of annealing involves inserting a holding time of t_e at $T = T_e$ during cooling. The time t_e is divided into ten subintervals to allow for the nonlinearity of enthalpy relaxation during annealing. A normalized heat capacity C_p^N, defined as dT_f/dT, has the values C_p(glass) = 0 and C_p(liquid) = 1.0. The method for normalizing the experimental data is described below.

Experimental Section

A single sample (20.1 mg) of Aldrich Secondary Standard polystyrene (lot 03) was dried at 130 °C for 2 h before being sealed in the DSC pan. The material is specified by the supplier as having $M_w = 3.21 \times 10^5$ and $M_n = 8.46 \times 10^4$. The sample was kept in the DSC instrument between runs, in an attempt to reduce experimental scatter due to differences in heat transfer effects. Measurements were performed on a Perkin-Elmer DSC-2 fitted with a Scanning Auto Zero module. Base line curvature was corrected at the only heating rate used, 10 K min^{-1}.

To monitor possible decomposition, a total of five rate cooling and reheating scans was run between the annealing experiments. For these, a cooling rate of −40 K min^{-1} from 420 to 300 K was followed immediately by reheating at 10 K min^{-1} over the same temperature range. For convenience, this thermal history will be referred to as −40/+10, with appropriate changes for other cooling rates. As a further test of reproducibility, three separate scans following 1-h anneals at 360 K were also run during the course of the experiments. In addition to serving as monitors of decomposition, these repeat experiments also provided a measure of experimental uncertainty which was used for evaluating the uncertainty in the model parameters obtained from the optimization procedure. Another sample of ca. 10 mg was also subjected to −40/+10 scans, to test for systematic thermal lag effects.

The experimental data were normalized by expressing the difference between the observed heat capacity C_p and the glassy heat capacity C_{pg} (linearly extrapolated into the transition region) as a fraction of the difference between the liquid heat capacity C_{pe} (similarly extrapolated) and C_{pg}. The temperature dependence of C_{pe} was always linear from 390 to 420 K, and extrapolation of C_{pe} into the transition region was not subject to significant uncertainty. In determining C_{pg}, however, care was taken to ensure that only the lowest temperature range (300 to ca. 330 K) was used. If a wider range was used, the slight exotherm just below the glass transition region caused a significant change in the slope of C_{pg}. This significantly affected only those data at the lower end of the glass transition, and most of the transition range, particularly the overshoot, is much less affected. In the five scans used to monitor decomposition, for example, the random scatter in the maximum of the overshoot, C_{pmax}, was much larger than the uncertainties introduced by the choice of C_{pg}.

To determine T_f' as a function of Q_C, scans at 10 K min^{-1} were recorded following cooling rates of −20, −10, and −5 K min^{-1}, in addition to the five −40/+10 runs. For each scan the normalized data were integrated up to temperatures at which the normalized heat capacity was unity, when $T_f = T$ and the integral is a linear function of T with unit slope. The temperature intercept of this linear function defines T_f'.

Annealing was performed during the cooling cycle to match the thermal history used in the calculations. Two sets of annealing experiments were performed. In the first, the annealing time was kept constant at 1 h and the annealing temperature was varied from 350 to 370 K in 5 K intervals. In the second set, the annealing temperature was held at 350 K and annealing performed for 4, 16, and 66 h. For both sets of experiments the cooling rate before and after annealing was 40 K min^{-1} and the reheating rate was 10 K min^{-1}. Cooling commenced at 420 K and stopped at 300 K, and reheating data were recorded over the same temperature range.

Optimization Procedure

Model parameters were obtained from the experimental data by a computer search using the Marquardt algorithm given by Kuester and Mize.[18] Predicted values of the normalized heat capacity, $\hat{C}_p(T)$, were obtained from the trial parameters, and the least-squares objective function, ψ, was defined as $\psi = \sum_T [C_p(T) - \hat{C}_p(T)]^2$, where $C_p(T)$ is the measured normalized heat capacity. The Marquardt algorithm minimizes ψ and allows for constraints on the search space for each parameter. For the present application x and β were constrained to lie between 0 and 1, the upper and lower bounds on A were input manually, and Δh^* was input as a constant. The optimum value of Δh^* was determined graphically from the minimum in ψ with respect to Δh^*. It was not possible to optimize all four parameters with the Marquardt program because A, Δh^*, and x are highly correlated. Although the best Δh^* might have been found by nesting two search routines, this was not attempted because of practical considerations of computer time.

Data Analysis

Optimum values of A, Δh^*, x, and β were obtained for each of the five −40/+10 runs and for a data set constructed from an average of the five normalized C_p values at each temperature. The averaged data set was assumed to represent the population of −40/+10 data sets, and the optimum set of parameters for it was used to predict the normalized C_p curves for other thermal histories.

Uncertainties in the best-fit parameters arise from two sources: (a) experimental scatter in the five runs and (b) uncertainties due to possible imperfect convergence of the Marquardt search. The parameter uncertainties due to experimental scatter were evaluated by comparing the optimum standard deviations for each of the five data sets with the deviation for the averaged data set, σ_{av}. The value of σ_{av} was assumed to represent the population and provided a basis for identifying any of the individual data sets as being unrepresentative of the population. An F test was used for this purpose. A data set was accepted as representative at the 95% confidence level if its standard deviation σ conformed to the F test inequality appropriate for the number of data points and degrees of freedom:

$$1/1.37 = 0.73 \leq (\sigma/\sigma_{av})^2 \leq 1.37 \quad (4)$$

The variation in parameters for the best fits to the rep-

Table I
Best-Fit Parameters

parameter	average	uncertainties due to: exptl scatter	uncertainties due to: fitting procedure	total uncertainty
$\Delta h^*/R$, K	8.25×10^4	$\pm 2.5 \times 10^3$	$\pm 5 \times 10^2$	$\pm 2.55 \times 10^3$
ln A (s)	−216.4	±8	±1	8.1
x	0.4255	±0.017	±0.035	±0.038
β	0.6767	±0.036	±0.023	±0.043

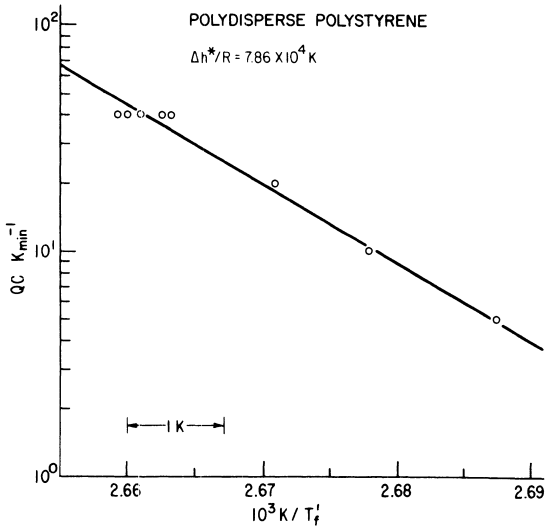

Figure 1. Experimental variation of $1/T_f'$ (see text for definition) with Q_C. Line is linear least-squares best fit and gives a value for $\Delta h^*/R$ of 7.86×10^4 K.

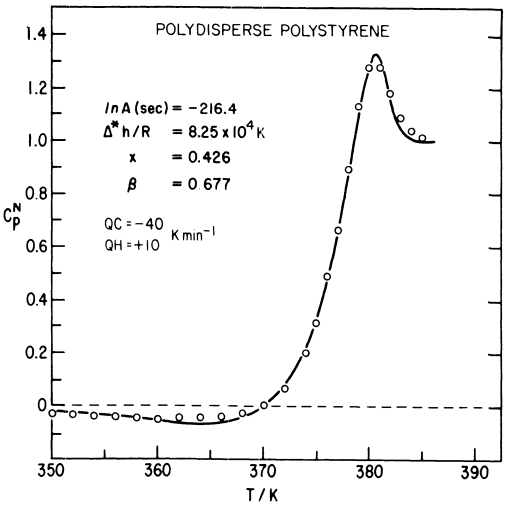

Figure 2. Optimum fit (line) to experimental C_p^N data (points) obtained by averaging five −40/+10 runs. The optimum value of $\Delta h^*/R$ agrees within uncertainty with the value obtained from Figure 1. Uncertainties in the parameters are given in Table I.

resentative data sets was assumed to reflect the experimental scatter.

Uncertainties associated with convergence of the Marquardt algorithm were estimated from a sensitivity analysis of the averaged data set. This was done by changing each parameter one at a time, with the other three held at their optimum values, and comparing the resulting standard deviation with σ_{av}. The maximum change in each parameter for which the inequality (4) remained valid was assumed to be the uncertainty associated with the fitting procedure. The total uncertainty was estimated as the square root of the sum of squares of the two sources of uncertainty for each parameter. This procedure gives a conservative estimate of the uncertainties in each of the optimum parameters, in the sense that if two or more of the parameters are held at their extreme values the best fit is unacceptably poor.

Results

From the variations in C_{pmax} for the five −40/+10 runs and the three 1-h anneals at 360 K, the random experimental uncertainty in the normalized heat capacity is estimated as ±5%. The results of −40/+10 scans with the 10-mg sample also agreed within this uncertainty, indicating no systematic thermal lag effects for this history. A plot of log Q_C vs. $1/T_f'$ is shown in Figure 1. Data for all five −40/+10 runs are included. The linear least-squares estimate of $\Delta h^*/R$ is 7.9×10^4 K, with an estimated uncertainty of $\pm 1.0 \times 10^4$ K.

In the statistical analysis of experimental uncertainty two of the −40/+10 runs were found to be unrepresentative and were rejected. The remaining three were used to estimate the uncertainties in the parameters. The optimum parameters and their uncertainties are given in Table I, and the optimum fit to the averaged −40/+10 data set is shown in Figure 2. The predicted curves for the −20/+10, −10/+10, and −5/+10 runs are compared with experimental points in Figure 3. A similar comparison

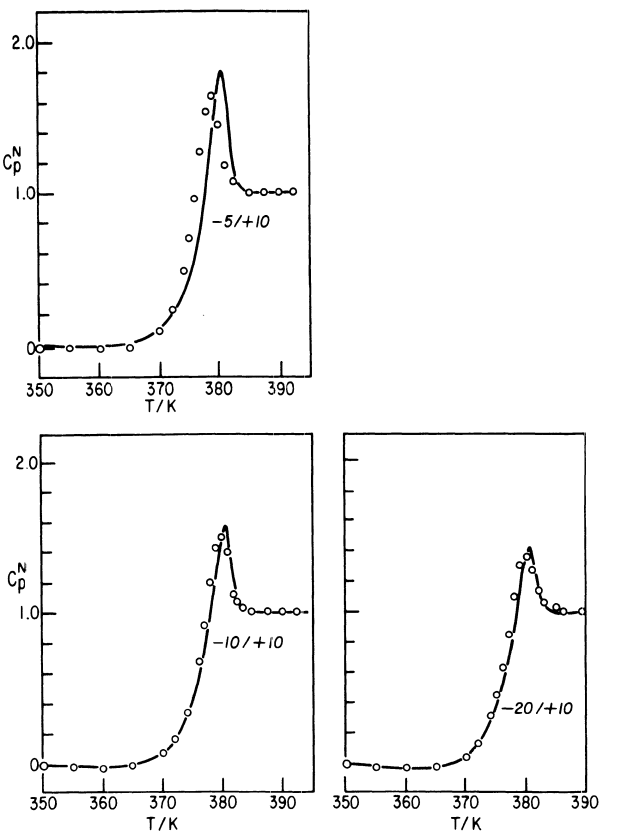

Figure 3. Predicted temperature dependence of C_p^N (lines) with cooling rate, using parameters determined from fit shown in Figure 2. Experimental data are shown as points.

is shown in Figure 4 for 1-h anneals at the indicated annealing temperatures. The data for the 360 K anneal are an average of the three experiments referred to above. Predicted curves and experimental points for anneals at

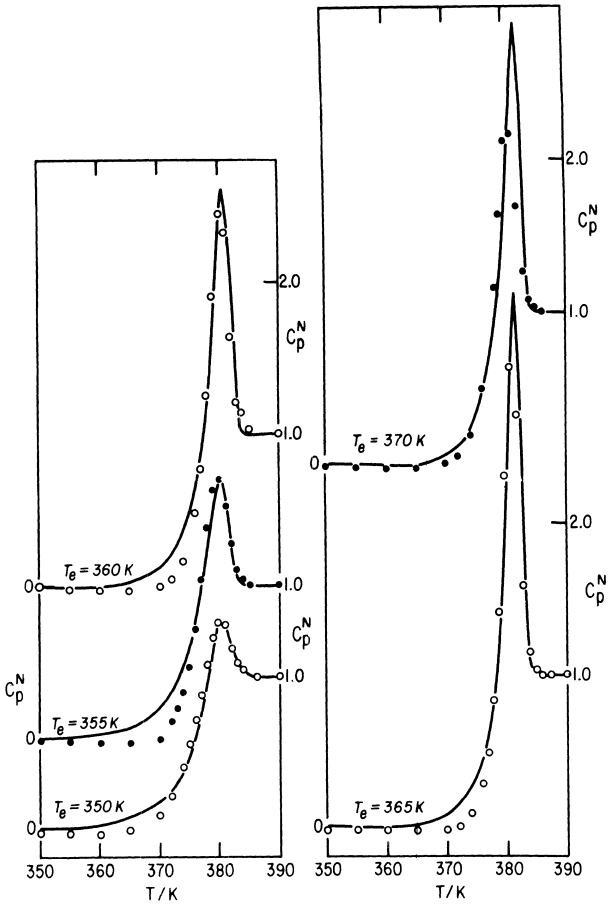

Figure 4. Predicted temperature dependence of C_p^N (lines) as a function of annealing temperature T_e from parameters determined from Figure 2. Annealing time is fixed at 1 h. Experimental data are shown as points (filled and unfilled circles are for clarity only).

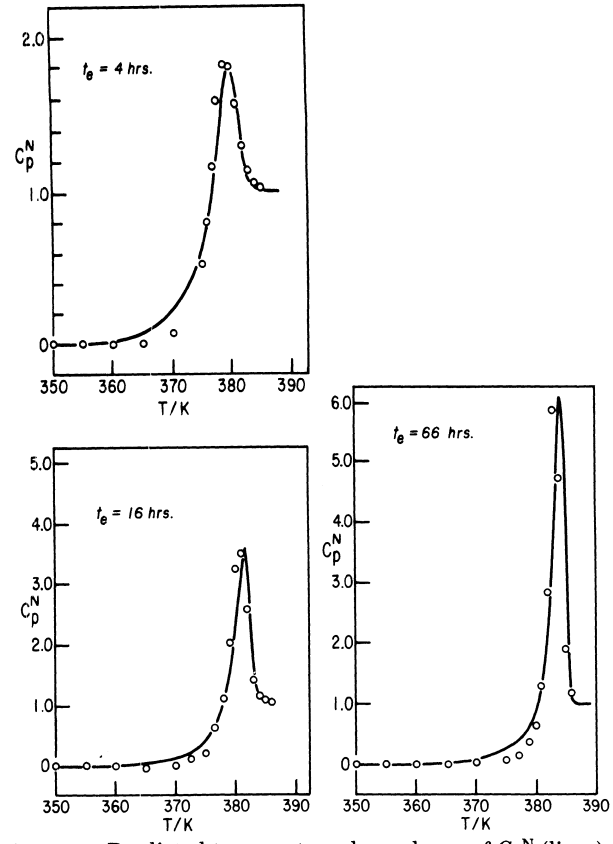

Figure 5. Predicted temperature dependence of C_p^N (lines) as a function of annealing time at 350 K from parameters determined from Figure 2. Experimental data are shown as points.

350 K for different annealing times are compared in Figure 5.

Discussion

The uncertainties estimated for x and β (0.038 and 0.043, Table I) compare favorably with those quoted by Moynihan (0.05 in each).[13] The agreement between the values of $\Delta h^*/R$ obtained directly from experiment ($(7.9 \pm 1.0) \times 10^4$ K, Figure 1), from the optimization procedure ($(8.25 \pm 0.25) \times 10^4$ K, Table I), and from analysis of data for a polydisperse polystyrene given by Wunderlich[19] (7.8×10^4 K) is strong evidence that the Marquardt algorithm works correctly. This is further supported by the reasonably good predictions of C_p for thermal histories which differ from that for which the parameters were determined. In particular, the generally good predictions of the effects of annealing demonstrate that the Moynihan formulation of the glass transition kinetics provides an adequate description of the effects of annealing on enthalpy relaxation for this material. Evidently the kinetic parameters that characterize the glass transition also determine the annealing behavior.

In view of the apparent validity of the model, it is of some interest to examine the implications of its approximations and assumptions. First, we discuss the approximation that Δh^* is independent of temperature. The justification for this in describing the glass transition kinetics is that the temperature range over which the glass transition occurs is sufficiently small that any variation in Δh^* is negligible. A similar claim can be made for the glassy-state behavior if the temperature T is replaced by the fictive temperature T_f, as suggested by Rusch[20] for applying the WLF equation to the glassy state, since the changes in T_f during annealing are for the most part comparable with the glass transition temperature range. The approximation that β is independent of T can be partially justified by the observation that the variation in β (typically 10–20% over a 30–40 K temperature range near T_g) is comparable with the uncertainties in the average. In any event, dependence of Δh^* or β on T and/or T_f is evidently not an essential feature of annealing and enthalpy relaxation, since experimental data are reproduced with reasonable accuracy when these parameters are assumed to be constant.

An implicit assumption is that the decrease in glassy heat capacity which sometimes occurs with annealing does not change the relaxation kinetics, since C_{pg} is removed by the normalization procedure. This is evidently true, since the effects of annealing can be predicted from the glass transition kinetics.

Numerical evaluation of the Boltzmann superposition integral also introduces approximations. It is assumed, for example, that temperature steps of 1 K are sufficiently small to ensure linearity. This has been shown by Moynihan to be adequate for describing the glass transition kinetics,[13] although its validity when very large changes in T_f occur (i.e., when the normalized heat capacity is much greater than 1, as occurs in annealed glasses) is questionable. Secondly, dividing the annealing time into 10 subintervals is arbitrary and there is an implicit assumption that this is a sufficient number. For the purpose of evaluating these two assumptions, calculations were repeated using a 0.5 K temperature steps and 40 subintervals for annealing. Approximations were considered adequate if the two calculations agreed to better than 5%, the estimated uncertainty for the experimental data. The as-

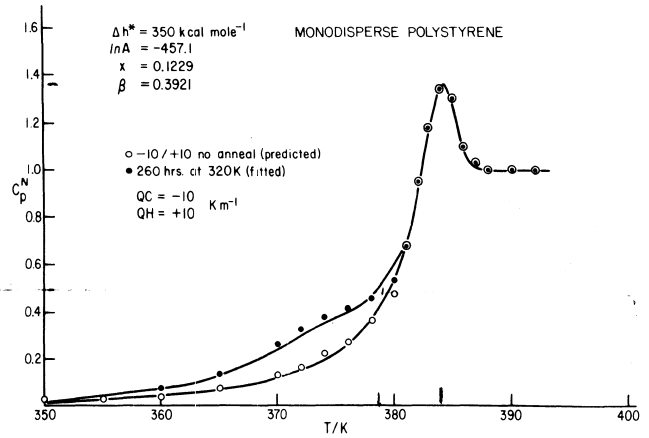

Figure 6. Fits to normalized experimental data (points) for monodisperse polystyrene.[23] Parameters optimized for history with 260-h anneal at 320 K (solid points). Curve for history with no annealing (open points) is predicted behavior. Original data have been normalized as described in text.

sumption that 1 K steps are sufficiently small appears to be valid when calculated values of C_p are less than ca. 2.5. At higher values of C_p, the calculations using 1 K steps produce C_p values that are lower than those produced by 0.5 K steps. The assumption that 10 subintervals for annealing are sufficient was found to be valid for values of t_e which were sufficiently small that T_f relaxed by less than ca. 2 K during each subinterval. When this condition was not met, the calculated values of C_{pmax} using 10 subintervals were higher than those calculated using 40 subintervals.

For the thermal histories considered here, only the prediction for the 66-h anneal at 350 K is significantly affected by the number of annealing subintervals. In this case, however, the use of 10 subintervals and temperature steps of 1 K give compensating changes in C_p and the calculated curve in Figure 5 is correct to within a few percent. The calculated curves for 1-h anneals at the highest values of T_e (365 and 370 K) are too low by ca. 5% because of the use of 1 K steps. When this is corrected for by using 0.5 K steps the calculated values of C_{pmax} exceed the experimental values by slightly more than the estimated random experimental uncertainty, suggesting that the best-fit parameters do not give an exact account of these high-T_e data. However, for these large overshoots thermal lag effects may reduce the observed overshoot, so that full agreement between the predictions and the corrected experimental data cannot be excluded. Discussions of thermal lag effects have been given by Lagasse[21] and Mraw.[22]

The Marquardt optimization procedure was also applied to data published by Chen and Wang[23] for a monodisperse polystyrene ($M_n = 2 \times 10^5$). Best-fit parameters were obtained from data for a single thermal history consisting of cooling at 10 K min^{-1}, annealing at 320 K for 260 h, and reheating at 10 K min^{-1}. They are ln A (s) = −457.1, $\Delta h^*/R = 1.75 \times 10^5$ K, $x = 0.12$, $\beta = 0.39$. The best fit is shown in Figure 6. The predicted curve for an unannealed glass with the same cooling and heating rates is also compared with experimental data in Figure 6. The fits to both histories are within the estimated uncertainties associated with transfer of the data from the published plots. The experimentally observed linear dependences of the enthalpy lost during annealing (ΔH) on (log t_e)^2 at $T_e = 320$ K and on log t_e at $T_e = 350$ K are also reproduced.

The best-fit parameters for the monodisperse and polydisperse polystyrenes analyzed here are markedly different. The lower value of x for the monodisperse material (0.12, compared with 0.43 for the polydisperse polymer) indicates that annealing effects should be more pronounced for the monodisperse material. It is perhaps surprising that the monodisperse material also has a broader distribution of relaxation times ($\beta = 0.39$ compared with 0.68). It is not clear why these differences are so large. Analysis of the molecular weight distribution of the polydisperse material indicated two log Gaussian components centered at 5×10^4 and 3×10^5 daltons, with weightings of 10% and 90%, respectively. Each component had a standard deviation of 1.1 log (dalton). The lowest molecular weight components therefore appear to be present in amounts too small to give a significant plasticizing effect. Although differences due to impurities cannot be ruled out, it would be surprising if they were so large. Analyses of many more data on the effects of molecular weight and molecular weight distribution are needed to resolve this question.

Summary

The effects of sub-T_g annealing on enthalpy relaxation in atactic, polydisperse, and monodisperse polystyrenes are well described by Moynihan's formulation of the glass transition kinetics. The optimization procedure used to obtain best-fit model parameters from experimental data is as accurate as the experimental data (±5% in the present case) and opens up the possibility of characterizing the enthalpy relaxation of amorphous materials in a routine manner.

Acknowledgment. This work was supported in part by National Science Foundation Grant No. CPE-7920740 under the Industry/University Cooperative Research Program. It is a pleasure to acknowledge the experimental assistance of D. Puraty and useful discussions with A. R. Berens and H. Hopfenberg. We thank H. S. Chen for providing preprints of ref 23. We thank The BFGoodrich Co. for permission to publish.

Registry No. Polystyrene, 9003-53-6.

References and Notes

(1) Illers, K.-H. *Makromol. Chem.* **1969**, *127*, 1.
(2) Weitz, A.; Wunderlich, B. *J. Polym. Sci., Polym. Phys. Ed.* **1974**, *12*, 2473.
(3) Gray, A.; Gilbert, M. *Polymer* **1976**, *17*, 44.
(4) Brown, I. G.; Wetton, R. E.; Richardson, M. J.; Savill, N. G. *Polymer* **1978**, *19*, 659.
(5) Richardson, M. J.; Savill, N. G. *Br. Polym. J.* **1979**, *11*, 123.
(6) Prest, W. M.; O'Reilly, J. M.; Roberts, F. J., Jr.; Mosher, R. A. *Polym. Prepr., Am. Chem. Soc., Div. Polym. Chem.* **1980**, *21* (2), 12. *Polym. Eng. Sci.*, in press.
(7) Wysgoski, M. G. *J. Appl. Polym. Sci.* **1980**, *25*, 1455.
(8) Foltz, C. R.; McKinney, P. V. *J. Appl. Polym. Sci.* **1969**, *13*, 2235.
(9) Ali, M. S.; Sheldon, R. P. *J. Appl. Polym. Sci.* **1970**, *14*, 2619.
(10) Petrie, S. E. B. *J. Polym. Sci., Part A-2* **1972**, *10*, 1255.
(11) Kovacs, A. J.; Aklonis, J. J.; Hutchinson, J. M.; Ramos, A. R. *J. Polym. Sci., Polym. Phys. Ed.* **1979**, *17*, 1097.
(12) Hodge, I. M.; Berens, A. R. *Macromolecules* **1982**, *15*, 762.
(13) DeBolt, M. A.; Easteal, A. J.; Macedo, P. B.; Moynihan, C. T. *J. Am. Ceram. Soc.* **1976**, *59*, 16.
(14) McCrum, N. G.; Read, B. E.; Williams, G. "Anelastic and Dielectric Effects in Polymeric Solids"; Wiley: New York, 1967.
(15) Tant, M. R.; Wilkes, G. L. *J. Appl. Polym. Sci.* **1981**, *26*, 2813.
(16) Menczel, J.; Wunderlich, B. *J. Polym. Sci., Polym. Lett. Ed.* **1981**, *19*, 261.
(17) Gardon, R.; Narayanaswamy, O. S. *J. Am. Ceram. Soc.* **1970**, *53*, 168.
(18) Kuester, J. L.; Mize, J. H. "Optimization Techniques with Fortran"; McGraw-Hill: New York, 1973.
(19) Wunderlich, B.; Bodily, D. M.; Kaplan, M. H. *J. Appl. Phys.* **1964**, *35*, 95.
(20) Rusch, K. C. *J. Macromol. Sci., Phys.* **1968**, *132*, 179.
(21) Lagasse, R. R. *J. Polym. Sci., Polym. Phys. Ed.* **1982**, *20*, 279.
(22) Mraw, S. C. *Rev. Sci. Instrum.* **1982**, *53*, 228.
(23) Chen, H. S.; Wang, T. T. *J. Appl. Phys.* **1981**, *52* (10), 5898.